COORDINATED SCIENCE LABORATORY
College of Engineering

AD-A197 723

DTIC FILE COPY

ELECTROMAGNETIC SCATTERING BY CONDUCTING BODIES OF REVOLUTION-- SOLUTION USING SUB-DOMAIN AND ENTIRE-DOMAIN BASIS FUNCTIONS

J. Joseph
R. Mittra

DTIC
ELECTE
AUG 1 6 1988
S   D
H

UNIVERSITY OF ILLINOIS AT URBANA-CHAMPAIGN

REPORT DOCUMENTATION PAGE

1a. REPORT SECURITY CLASSIFICATION	1b. RESTRICTIVE MARKINGS
Unclassified	None

2a. SECURITY CLASSIFICATION AUTHORITY	3. DISTRIBUTION / AVAILABILITY OF REPORT
	Approved for public release;
2b. DECLASSIFICATION / DOWNGRADING SCHEDULE	distribution unlimited

4. PERFORMING ORGANIZATION REPORT NUMBER(S)	5. MONITORING ORGANIZATION REPORT NUMBER(S)
UILU-ENG-88-2240	

6a. NAME OF PERFORMING ORGANIZATION	6b. OFFICE SYMBOL (If applicable)	7a. NAME OF MONITORING ORGANIZATION
Coordinated Science Lab University of Illinois	N/A	Office of Naval Research

6c. ADDRESS (City, State, and ZIP Code)	7b. ADDRESS (City, State, and ZIP Code)
1101 W. Springfield Ave. Urbana, IL 61801	800 N. Quincy St. Arlington, VA 22217

8a. NAME OF FUNDING / SPONSORING ORGANIZATION Joint Services Electronics Program	8b. OFFICE SYMBOL (If applicable)	9. PROCUREMENT INSTRUMENT IDENTIFICATION NUMBER
		N00014-84-C-0149

8c. ADDRESS (City, State, and ZIP Code)	10. SOURCE OF FUNDING NUMBERS			
	PROGRAM ELEMENT NO.	PROJECT NO.	TASK NO.	WORK UNIT ACCESSION NO
800 N. Quincy St. Arlington, VA 22217				

11. TITLE (Include Security Classification)
Electromagnetic Scattering by Conducting Bodies of Revolution - Solution Using Sub-Domain and Entire-Domain Basis Functions.

12. PERSONAL AUTHOR(S)
Joseph, J. and Mittra, R.

13a. TYPE OF REPORT	13b. TIME COVERED	14. DATE OF REPORT (Year, Month, Day)	15. PAGE COUNT
Technical	FROM _____ TO _____	1988 August	36

16. SUPPLEMENTARY NOTATION

17. COSATI CODES			18. SUBJECT TERMS (Continue on reverse if necessary and identify by block number)
FIELD	GROUP	SUB-GROUP	electromagnetic scattering; method of moments; bodies of revolution; entire-domain functions; sub-domain functions.

19 ABSTRACT (Continue on reverse if necessary and identify by block number)

In this work, the problem of electromagnetic scattering of a plane wave incident on a conducting body of revolution is considered. The body is assumed to be situated in infinite homogeneous space. The problem is solved using the method of moments. Use of two different types of expansion and testing functions, namely, sub-domain type and entire-domain type is considered. Results obtained using sub-domain pulse functions and entire-domain Gaussian functions are presented. The relative advantages and disadvantages of each type of basis functions is discussed.

20. DISTRIBUTION / AVAILABILITY OF ABSTRACT	21. ABSTRACT SECURITY CLASSIFICATION
☒ UNCLASSIFIED/UNLIMITED ☐ SAME AS RPT. ☐ DTIC USERS	Unclassified
22a. NAME OF RESPONSIBLE INDIVIDUAL	22b. TELEPHONE (Include Area Code) 22c. OFFICE SYMBOL

DD FORM 1473, 84 MAR

83 APR edition may be used until exhausted
All other editions are obsolete.

ELECTROMAGNETIC SCATTERING BY
CONDUCTING BODIES OF REVOLUTION

SOLUTION USING
SUB-DOMAIN AND ENTIRE-DOMAIN
BASIS FUNCTIONS

by

J. Joseph and R. Mittra
Electromagnetic Communication Laboratory
University of Illinois
Urbana, Illinois

Abstract

In this work, the problem of electromagnetic scattering of a plane wave incident on a conducting body of revolution is considered. The body is assumed to be situated in infinite homogeneous space. The problem is solved using the method of moments. Use of two different types of expansion and testing functions, namely, sub-domain type and entire-domain type is considered. Results obtained using sub-domain pulse functions and entire-domain Gaussian functions are presented. The relative advantages and disadvantages of each type of basis functions is discussed.

Table of Contents

List of Figures

List of Tables

INTRODUCTION

The problem of electromagnetic scattering by a conducting body of revolution, illuminated by a plane wave incident from some arbitrary direction is considered. The geometry of the problem is shown in Fig.1. The body is generated by the arc C revolving around the z-axis.

The objective is to compute the scattered far fields and radar cross-section of the body of revolution. In this paper, the electric field integral equation which enforces the total tangential electric fields on the surface of the body to be zero is used to solve the problem. First, equivalent electric currents are postulated on the surface of the body. The scattered field is expressed in terms of these equivalent currents. The electric field integral equation is then solved numerically to obtain the surface currents. The surface currents are then used to obtain the radar cross-section and far-fields.

The numerical solution of the integral equation is obtained using the method of moments. First, the surface currents are expanded in a set of appropriate basis functions. The resulting equation is then tested with a set of weighting functions to obtain a matrix equation with the coefficients of the currents as unknowns.

The currents are expanded in a Fourier series in the azimuthal (ϕ) direction and tested with the conjugates of these expansion functions. This results in the decoupling of the equations of various azimuthal modes. The advantage of this is that one can solve several smaller matrices corresponding

to a two dimensional problem and combine these solutions to obtain the solution for the body of revolution problem.

There are several possible choices of the expansion/testing functions in the t-direction(the axial direction - see Fig. 1) for the current. In this paper, two classes of expansion functions namely, sub-domain and entire-domain functions are considered. Two programs, PBOR and GBOR have been developed. PBOR uses sub-domain pulse basis functions and testing functions. GBOR uses entire-domain Gaussian basis and testing functions. The advantages and disadvantages of each of these approaches as well as some numerical examples are presented.

FORMULATION

Consider a conducting body of revolution situated in homogeneous space as shown in Fig. 1. The body is illuminated by a plane wave incident from some arbitrary angle. The total electric field at any point in space is the sum of the incident field and the field scattered by the body. The total field tangential to the surface of the conducting body is zero. That is,

$$\hat{n} \times \mathbf{E}^{total} = \hat{n} \times [\mathbf{E}^{inc} + \mathbf{E}^{scat}] = 0 \tag{1}$$

on the surface of the body. In (1), $\mathbf{E}^{inc}$ is the incident electric field, $\mathbf{E}^{scat}$ is the scattered field, and $\mathbf{n}$ is the outward pointing normal unit vector on the surface of the scatterer (see Fig. 1). Using equivalence principle, the scatterer can be replaced with a surface electric current $\mathbf{J}$ radiating in homogeneous space. The scattered field of (1) can then be expressed in terms of these equivalent currents as

$$\mathbf{E}^{scat}(\mathbf{r}) = -j\omega\mathbf{A}(\mathbf{r}) - \nabla\Phi(\mathbf{r}) \tag{2}$$

with the potentials of (2) given by

$$\mathbf{A}(\mathbf{r}) = \frac{\mu}{4\pi}\iint_S \mathbf{J}(\mathbf{r}')G(\mathbf{r}, \mathbf{r}')dS' \tag{3}$$

and

$$\Phi = \frac{1}{4\pi\varepsilon}\iint_S \rho(\mathbf{r}')G(\mathbf{r}, \mathbf{r}')dS' \tag{4}$$

In (3) and (4), μ and ε are the parameters of the homogeneous space and S denotes the surface of the scatterer. The charge density $\rho(\mathbf{r}')$ of (4) can be expressed in terms of the surface current $\mathbf{J}$ as

$$\rho(\mathbf{r}') = \frac{j}{\omega}[\nabla_s \cdot \mathbf{J}(\mathbf{r}')] \tag{5}$$

The subscript s on the divergence operator denotes surface divergence. The homogeneous space Greens function G used in (3) and (4) is defined as

$$G(\mathbf{r}, \mathbf{r}') = \frac{e^{-jkR}}{R} \tag{6}$$

with R being the distance between an observation point $\mathbf{r} = (\rho, \phi, z)$ and a source point $\mathbf{r}' = (\rho', \phi', z')$. In cylindrical coordinates it is computed as

$$R = |\mathbf{r} - \mathbf{r}'| = \sqrt{\rho^2 + \rho'^2 - 2\rho\rho'\cos(\phi - \phi') + (z - z')^2} \tag{7}$$

Now we can combine (1) through (7) to get an integral equation as shown below.

$$\hat{n} \times \mathbf{E}^{inc} = \hat{n} \times \left\{ \frac{j\omega}{4\pi} \iint_S \mathbf{J}(\mathbf{r}')G(\mathbf{r}, \mathbf{r}')dS' + \frac{j}{4\pi\omega}\nabla \int_S \int (\nabla_s \cdot \mathbf{J}(\mathbf{r}'))G(\mathbf{r}, \mathbf{r}')dS' \right\} \tag{8}$$

Our objective now is to solve this integral equation for the equivalent surface current $\mathbf{J}$. This current can be used to obtain other quantities of interest such as scattered far-fields or radar cross-section. To obtain a solution, first we express the vector surface current of (8) as the sum of two orthogonal components on the surface

$$\mathbf{J} = \hat{\phi}J_\phi + \hat{t}J_t \tag{9}$$

Here ϕ is the unit vector on the surface of the body, in the cylindrical coordinate system of Fig. 1, and $\mathbf{t}$ is a unit vector on the surface of the body such that $(\mathbf{n}, \phi, \mathbf{t})$ form a right hand triad. The incident field $\mathbf{E}^{inc}$ of (8) also can be expressed as the sum of its ϕ and $\mathbf{t}$ components. Thus (8) can be written in component operator form as

$$
\begin{bmatrix} E_t^{inc} \\ E_\phi^{inc} \end{bmatrix} = \begin{bmatrix} \beta_{11} & \beta_{12} \\ \beta_{21} & \beta_{22} \end{bmatrix} \begin{bmatrix} J_t \\ J_\phi \end{bmatrix} \tag{10}
$$

The β_{ij}'s are integro-differential operators operating on the appropriate components of current. These are obtained by computing the dot product of (8) with appropriate unit vectors and separating out the J_ϕ part and J_t part. The explicit expressions for these operators are shown below

$$
\beta_{11}(J_t) = \frac{j\omega\mu}{4\pi} \iint_S J_t \{\sin\gamma \sin\gamma' \cos(\phi'-\phi) + \cos\gamma \cos\gamma'\} G dS'
$$

$$
+ \frac{j}{4\pi\omega\varepsilon} \frac{\partial}{\partial t} \iint_S \frac{\partial}{\rho'\partial t'}(\rho' J_t) G dS' \tag{11a}
$$

$$
\beta_{12}(J_\phi) = -\frac{j\omega\mu}{4\pi} \iint_S J_\phi \sin\gamma \sin(\phi'-\phi) G dS' + \frac{j}{4\pi\omega\varepsilon} \frac{\partial}{\partial t} \iint_S \frac{\partial}{\rho'\partial\phi'}(J_\phi) G dS' \tag{11b}
$$

$$
\beta_{21}(J_t) = \frac{j\omega\mu}{4\pi} \iint_S J_t \sin\gamma' \sin(\phi'-\phi) G dS' + \frac{j}{4\pi\omega\varepsilon\rho} \frac{\partial}{\partial\phi} \iint_S \frac{\partial}{\rho'\partial t'}(\rho' J_t) G dS' \tag{11c}
$$

$$\beta_{22}(J_\phi) = \frac{j\omega\mu}{4\pi}\iint_S J_\phi \cos(\phi'-\phi)GdS' + \frac{j}{4\pi\omega\epsilon\rho}\frac{\partial}{\partial\phi}\iint_S \frac{\partial}{\rho'\partial\phi'}(J_\phi)GdS'$$

(11d

In these equations, the primed coordinates refer to the source points on the surface of the scatterer and the unprimed coordinates refer to the observation points. The angle γ is the angle the tangent vector t makes with the axis of the body. This angle is taken to be positive if the tangent vector points away from the axis of the body and negative if it points towards the axis. The surface divergence in surface coordinates given by

$$\nabla_{s'}\cdot\mathbf{J} = \frac{\partial}{\rho'\partial t'}(\rho'J_t) + \frac{\partial}{\rho'\partial\phi'}(J_\phi)$$

has been used to obtain (11).

To obtain a solution for the unknown currents J_t and J_ϕ of (11), the method of moments is used. The first step in the solution procedure is to express the current using a set of suitable basis functions as shown below.

$$\mathbf{J}(t,\phi) = \hat{\phi}J_\phi(t,\phi) + \hat{t}J_t(t,\phi)$$

(12a

$$= \hat{\phi}\sum_{m=-\infty}^{\infty}\sum_{n=1}^{N_\phi}J_\phi^{mn}U_\phi^n(t')e^{jm\phi} + \hat{t}\sum_{m=-\infty}^{\infty}\sum_{n=1}^{N_t}J_t^{mn}U_t^n(t')e^{jm\phi}$$

(12b

$$= \hat{\phi}\sum_{m=-\infty}^{\infty}\sum_{n=1}^{N_\phi}J_\phi^{mn}U_\phi^n(t')e^{jm\phi} + \frac{\hat{t}}{2\pi\rho'}\sum_{m=-\infty}^{\infty}\sum_{n=1}^{N_t}I_t^{mn}U_t^n(t')e^{jm\phi}$$

(12c

Here the J's are the unknown coefficients of current yet to be determined. N_ϕ and N_t are the number of basis functions used to expand J_ϕ and J_t respectively. I_t^{mn} of (12c) is defined as

$$I_t^{mn} = 2\pi\rho' J_t^{mn}$$

(12d

The reason for solving for I_t^{mn} rather than J_t^{mn} will be discussed later.

In (12), the azimuthal variation of the currents has been expanded in a Fourier series. The basis functions used for expansion in the orthogonal (**t**) direction are denoted by the U's. These basis functions can either be sub-domain or entire-domain basis functions. In this paper, one of each kind is considered. Sub-domain pulse basis functions with the necessary derivatives approximated using finite differencing and entire-domain Gaussian basis functions are considered.

Next step in the solution process is to test the equations with a set of suitable weighting functions to obtain a matrix equation. Following Galerkin's method, we test with the conjugates of the expansion functions. That is,

$$T_t^{pq} = T_t^q e^{-jp\phi} = U_t^q(t)e^{-jp\phi}, \qquad q=1,\cdots,N_t \tag{13a}$$

$$T_\phi^{pq} = T_\phi^q e^{-jp\phi} = U_\phi^q(t)e^{-jp\phi}, \qquad q=1,\cdots,N_\phi \tag{13b}$$

(12a) is used to test the first row of (10) and (12b) is used to test the second row.

To obtain the expressions for the matrix elements, the Greens function G appearing in (11) is expanded in a Fourier series as shown below.

$$\frac{e^{-jkR}}{R} = \frac{1}{2\pi} \sum_{m=-\infty}^{\infty} G_m e^{m(\phi-\phi')} \tag{14a}$$

where

$$G_m = \int_{-\pi}^{\pi} \frac{e^{-jkR}}{R} \cos(m\xi)\, d\xi \tag{14b}$$

with R defined in (7) with $(\phi-\phi')$ replaced with ξ.

Testing (10) with (13) now decouples the equations for various azimuthal modes m. The integrations in ϕ and ϕ' can be carried out analytically. The integrations in t and t' must be done numerically. Also, the Greens function G_m is an integral. Thus a three dimensional numerical integration is required to obtain the matrix elements corresponding to β.

The generating arc C in Fig.1 over which the t and t' integrations are to be performed are in general arbitrarily shaped. For computational purposes, this curve is approximated as linear segments connected end to end as shown in Fig. 2. Then, the integrations in t and t' must be carried out over each of these segments. To reduce the computational effort, we can approximate the t integral by evaluating the integrand only on one point per linear segment of the generating arc. This is equivalent to doing point matching when the testing function spans only one linear segment, such as is the case when pulse basis functions are used. Since this integration is carried out over the incident field which is a smoothly varying quantity, this approximation does not introduce significant error if the scatterer is modeled with sufficient number of linear segments. The resulting expressions for the various β's for azimuthal mode m are given below. The first summation is over the field segments and the second summation is over the source segments. The total number of linear segments is F and the s'th linear segment extends from t_{s-1} to t_s.

$$\beta_{11}^{qn} = \frac{j\omega\mu}{8\pi} \sum_{f=1}^{F} \Delta t_f \, T_t^q(t_{f-1/2}) \sin \gamma_f$$

$$\sum_{s=1}^{F} \sin \gamma_s' \left\{ \int_{t_{s-1}}^{t_s} dt' U_t^n(t_{s'}) \, G_{m+1}(t_{f-1/2}) + \int_{t_{s-1}}^{t_s} dt' U_t^n(t_{s'}) \, G_{m-1}(t_{f-1/2}) \right\}$$

$$+ \frac{j\omega\mu}{4\pi} \sum_{f=1}^{F} \Delta t_f T_t^q(t_{f-1/2}) \cos \gamma_f \sum_{s=1}^{F} \cos \gamma_s' \int_{t_{s-1}}^{t_s} dt' U_t^n(t_{s'}) \, G_m(t_{f-1/2})$$

$$- \frac{j}{4\pi\omega\varepsilon} \sum_{f=1}^{F} \Delta t_f \, \frac{d}{dt}[T_t^q(t_{f-1/2})] \sum_{s=1}^{F} \int_{t_{s-1}}^{t_s} dt' \, \frac{d}{dt'}[U_t^n(t_s')] \, G_m(t_{f-1/2})$$

$$q = 1, 2, \cdots, N_t$$

$$n = 1, 2, \cdots, N_t \qquad (15a)$$

$$\beta_{12}^{qn} = \frac{-\omega\mu}{4} \sum_{f=1}^{F} \Delta t_f \, T_t^q(t_{f-1/2}) \sin \gamma_f$$

$$\sum_{s=1}^{F} \left\{ \int_{t_{s-1}}^{t_s} dt' \rho' U_\phi^n(t_s') \, G_{m+1}(t_{f-1/2}) - \int_{t_{s-1}}^{t_s} dt' \rho' U_\phi^n(t_s') \, G_{m-1}(t_{f-1/2}) \right\}$$

$$+ \frac{jn}{2\omega\varepsilon} \sum_{f=1}^{F} \Delta t_f \, \frac{d}{dt}[\, T_t^q(t_{f-1/2}) \,] \sum_{s=1}^{F} \int_{t_{s-1}}^{t_s} dt' \, U_\phi^n(t_s') \, G_m(t_{f-1/2})$$

$$q = 1, 2, \cdots, N_t$$

$$n = 1, 2, \cdots, N_\phi \qquad (15b)$$

$$\beta_{11}^{qn} =$$

$$\beta_{21}^{qn} = \frac{-\omega\mu}{9\pi} \sum_{f=1}^{F} \Delta t_f \; \rho_{f-1/2} T_\phi^q(t_{f-1/2})$$

$$\sum_{s=1}^{F} \sin \gamma_{s'} \left\{ \int_{t_{s-1}}^{t_s} dt' U_t^n(t_s') \; G_{m+1}(t_{f-1/2}) - \int_{t_{s-1}}^{t_s} dt' U_t^n(t_s') \; G_{m-1}(t_{f-1/2}) \right\}$$

$$- \frac{m}{4\pi\omega\varepsilon} \sum_{f=1}^{F} \Delta t_t \; T_\phi^q(t_{f-1/2}) \sum_{s=1}^{F} \int_{t_{s-1}}^{t_s} dt' \; \frac{d}{dt'} \; U_t^n(t') \; G_m(t_{f-1/2})$$

$$q = 1, 2, \cdots, N_\phi$$

$$n = 1, 2, \cdots, N_t \qquad (15c)$$

$$\beta_{22}^{qn} = \frac{j\omega\mu}{4} \sum_{f=1}^{F} \Delta t_f \; \rho_{f-1/2} \; T_\phi^q(t_{f-1/2})$$

$$\sum_{s=1}^{F} \left\{ \int_{t_{s-1}}^{t_s} dt' \rho' U_\phi^n(t_s') \; G_{m+1}(t_{f-1/2}) + \int_{t_{s-1}}^{t_s} dt' \rho' U_\phi^n(t_s') \; G_{m-1}(t_{f-1/2}) \right\}$$

$$- \frac{jm^2}{2\omega\varepsilon} \sum_{f=1}^{F} \Delta t_f \; T_\phi^q(t_{f-1/2}) \sum_{s=1}^{F} \int_{t_{s-1}}^{t_s} dt' \; U_\phi^n(t_s') \; G_m(t_{f-1/2})$$

$$q = 1, 2, \cdots, N_\phi$$

$$n = 1, 2, \cdots, N_\phi \qquad (15d)$$

The integrals of (15) have a singularity in the integrand when the source point coincides with the field point. For a discussion of the handling of the singular terms, see [2].

As discussed earlier, the basis functions U_ϕ and U_t can be either sub-domain or entire-domain functions. In the next section, pulse basis functions which are of the sub-domain type is considered.

Sub-domain pulse basis functions

Fig. 3 shows the arrangement of pulse basis functions used in this paper. P_ϕ's are used for the ϕ component of current and P_t's are used for the t component. They are defined as follows

$$U_\phi^n(t) = P_\phi^s(t) = \begin{cases} 1 & t_{s-1} \leq t \leq t_s \\ \\ 0 & \text{otherwise} \end{cases} \tag{16a}$$

$$U_t^n(t) = P_t^s(t) = \begin{cases} 1 & t_{s-1/2} \leq t \leq t_{s-1/2} \\ \\ 0 & \text{otherwise} \end{cases} \tag{16b}$$

Observe that the U_ϕ^s is confined to the s'th linear segment. Thus there are a total of F of these basis functions. That is, $N_\phi = F$. On the other hand, we have chosen the U_t^s to straddle over two linear segments. There are a total of F-1 of these, which implies that $N_t = F-1$. The first half of the first sub-section and the last half of the last sub-section is assumed to have zero t-directed current. This is not a correct assumption if we are considering the current densities for a scatterer such as the one in Fig. 1. However, we can solve for $I_t = 2\pi\rho J_t$, rather than J_t itself. In this case, I_t will be close to zero near the points where the generating approaches the axis, by virtue of ρ approaching zero. This is the reason for

expanding the currents using I_t rather than using J_t in (12c).

As mentioned previously, the testing functions used are conjugates of the expansion functions. Since the pulse basis and testing functions are confined to a small region of the generating arc of Fig. 2, most of the terms of the double summation of (14) will drop out. The resulting expressions can be simplified as shown in (18). In obtaining these expressions, the derivative of U_t has been computed using finite differencing as

$$\frac{\partial}{\partial t'}(U_t^n(t')) = \frac{U_\phi^n(t')-U_\phi^{n+1}(t')}{0.5*(\Delta t_{n+1}+\Delta t_n)} \tag{17}$$

As mentioned earlier, the t integration is performed by doing one function evaluation per linear segment. This turns out to be one function evaluation per testing function. These function evaluations are done at the center of each testing function. The expressions for the elements of the moment matrix for azimuthal mode m using pulse basis functions are given on the following pages.

$$\beta_{11}^{qn} = \frac{j\omega\mu}{8\pi}\chi_s(\Delta t_q, \gamma_q)\sin\gamma_n' \ \{\psi(t_{n-1/2}, t_n, t_q, m+1)+\psi(t_{n-1/2}, t_n, t_q, m-1)\}$$

$$+ \ \frac{j\omega\mu}{8\pi}\chi_s(\Delta t_q, \gamma_q)\sin\gamma_{n+1}' \ \{\psi(t_n, t_{n+1/2}, t_q, m+1)+\psi(t_n, t_{n+1/2}, t_q, m-1)\}$$

$$+ \ \frac{j\omega\mu}{4\pi}\chi_c(\Delta t_q, \gamma_q) \ \{\cos\gamma_n'\psi(t_{n-1/2}, t_n, t_q, m) \ + \ \cos\gamma_{n+1}'\psi(t_n, t_{n+1/2}, t_q, m)\}$$

$$- \ \frac{j}{4\pi\omega\epsilon\Delta t_{n+1}}\{\psi(t_n, t_{n+1}, t_{q+1/2}, m)-\psi(t_n, t_{n+1}, t_{q-1/2}, m)\}$$

$$+ \ \frac{j}{4\pi\omega\epsilon\Delta t_n}\{\psi(t_{n-1}, t_n, t_{q+1/2}, m)-\psi(t_{n-1}, t_n, t_{q-1/2}, m)\} \tag{18a}$$

$$n=1, \cdots, F-1$$
$$q=1, \cdots, F-1$$

$$\beta_{12}^{qn} = \frac{-\omega\mu}{4}\chi_s(\Delta t_q, \gamma_q)\{\psi^\rho(t_{n-1}, t_n, t_q, m+1)-\psi^\rho(t_{n-1}, t_n, t_q, m-1)\}$$

$$+ \ \frac{m}{2\omega\epsilon}\{\psi(t_{n-1}, t_n, t_{q-1/2}, m)-\psi(t_{n-1}, t_n, t_{q+1/2}, m)\} \tag{18b}$$

$$n=1, \cdots, F$$
$$q=1, \cdots, F-1$$

$$\beta_{21}^{qn} = \frac{\omega\mu\Delta t_q \sin\gamma_n'}{8\pi}\{\psi(t_{n-1/2}, t_n, t_{q-1/2}, m+1) - \psi(t_{n-1/2}, t_n, t_{q-1/2}, m-1)\}$$

$$+ \frac{\omega\mu\Delta t_q \sin\gamma_{n+1}'}{8\pi}\{\psi(t_n, t_{n+1/2}, t_{q-1/2}, m+1) - \psi(t_n, t_{n+1/2}, t_{q-1/2}, m-1)\}$$

$$+ \frac{m\Delta t_q}{4\pi\omega\epsilon\rho_{q-1/2}\Delta t_{n+1}}\psi(t_n, t_{n+1}, t_{q-1/2}, m) - \frac{m\Delta t_q}{4\pi\omega\epsilon\rho_{q-1/2}\Delta t_n}\psi(t_{n-1}, t_n, t_{q-1/2}, m)$$

$$n = 1, \cdots, F-1 \qquad (18c)$$

$$q = 1, \cdots, F$$

$$\beta_{22}^{qn} = \frac{j\omega\mu\Delta t_q}{4}\{\psi^\rho(t_{n-1}, t_n, t_q, m+1) + \psi^\rho(t_{n-1}, t_n, t_{q-1/2}, m-1)\}$$

$$- \frac{jm^2\Delta t_q}{2\omega\epsilon\rho_{q-1/2}}\psi(t_{n-1}, t_n, t_{q-1/2}, m) \qquad (18d)$$

$$n = 1, \cdots, F$$

$$q = 1, \cdots, F$$

The various quantities used in (18) are defined in (19) and (20) below, and in Figs. 2 and 3.

$$\psi(t_1, t_2, t_q, m) = \int_{t_1}^{t_2} G_m(t_q, t')dt' \qquad (19)$$

with G_m defined in (14) and (7). The χ's of (18) are defined as

$$\chi_s(\Delta t_q, \gamma_q) = \frac{\Delta t_{q+1}\sin\gamma_{q+1} + \Delta t_q\sin\gamma_q}{2} \tag{20a}$$

$$\chi_c(\Delta t_q, \gamma_q) = \frac{\Delta t_{q+1}\cos\gamma_{q+1} + \Delta t_q\cos\gamma_q}{2} \tag{20b}$$

Entire-domain Gau ;ian basis functions

Each function of an entire-domain basis set, unlike the sub-domain basis functions, span the entire structure. The example used here is Gaussian functions as shown in Fig. 4. The n'th basis function is centered at μ_n (the mean). The "thickness" of the basis function is determined by its variance σ_n. The mathematical expressions that describe the functions of Fig. 4 are given below.

$$U_\phi^n(t) = U_t^n(t) = G^n(t) = \begin{cases} e^{-0.5\left(\frac{\mu_n - t}{\sigma}\right)^2} & t_L \leq t \leq t_U \\ e^{-0.5\left(\frac{\mu_n - t_L}{\sigma}\right)^2}\dfrac{t}{t_L} & 0 \leq t \leq t_L \\ e^{-0.5\left(\frac{\mu_n - (R - t_U)}{\sigma}\right)^2}\dfrac{R - t_U}{t_L} & t_U \leq t \leq R \end{cases} \tag{20}$$

In these expressions, the quantity R is the length of the generating arc. t_L and t_U are points on the generating arc. t_L is near $t=0$ (the beginning of the generating arc) and t_U is rear $t=R$ (end of the generating arc). The basis functions are forced to go to zero linearly between t_L and 0, and between t_U and R.

The basis functions used for both J_t and J_ϕ are the same and are given in (20). However, for J_ϕ the number of basis functions used is two more than that used for J_t. These two

extra basis functions are also Gaussian basis functions described by (20) and are centered at $t=0$ and $t=R$.

The derivatives of basis and testing functions with respect t required in (15) are easily computed from (20) and are given below.

$$\frac{\partial}{\partial t} G^n(t) = \begin{cases} \dfrac{\mu_n-t}{\sigma^2} e^{-0.5\left(\frac{\mu_n-t}{\sigma}\right)^2} & t_L \leq t \leq t_U \\[3ex] e^{-0.5\left(\frac{\mu_n-t_L}{\sigma}\right)^2} \dfrac{1}{t_L} & 0 \leq t \leq t_L \\[3ex] e^{-0.5\left(\frac{\mu_n-(R-t_U)}{\sigma}\right)^2} \dfrac{(-1)}{(R-t_U)} & t_U \leq t \leq R \end{cases} \tag{21}$$

Unlike the sub-domain basis set where the number of basis functions was linked to the number of linear segments used to model the scatterer, the number of entire-domain basis functions used have no relationship to the number of segments on the generating arc. However, since the t integrations in (15) have been performed by evaluating the integrand at one point per linear segment, the accuracy of computations are dependent on the number of linear segments.

Since each function of the basis set extends over the entire span of the scattering structure, the integrations required to obtain the expressions for β's must be carried out over the entire structure. This causes the computation time required to obtain a solution using the entire-domain basis set to be considerably larger than that using sub-domain basis set. However, using the entire-domain basis set one can obtain about the same degree of accuracy in solution

by solving a smaller matrix than would be required if sub-domain basis set were used.

Incident field

An arbitrarily polarized incident plane wave field $\mathbf{E}^{inc}$ is expressed as the sum of two linearly polarized plane waves as

$$\mathbf{E}^{inc} = (E_\theta^{inc}\hat{\theta}^{inc} + E_\phi^{inc}\hat{\phi}^{inc}) \, e^{-jk\hat{n}\cdot\mathbf{r}} \tag{22}$$

where

$$\hat{\theta}^{inc} = \cos\theta^{inc}\cos\phi^{inc}\hat{x} + \cos\theta^{inc}\sin\phi^{inc}\hat{y} - \sin\theta^{inc}\hat{z} \tag{23a}$$

$$\hat{\phi}^{inc} = -\sin\phi^{inc}\hat{x} + \cos\phi^{inc}\hat{y} \tag{23b}$$

$$\hat{n} = -\sin\theta^{inc}\cos\phi^{inc}\hat{x} - \sin\theta^{inc}\sin\phi^{inc}\hat{y} - \cos\theta^{inc}\hat{z} \tag{23c}$$

$$\mathbf{r} = \rho\cos\phi \, \hat{x} + \rho\sin\phi \, \hat{y} + z\hat{z} \tag{23c}$$

The elements of the forcing function vector in (10) are found by finding the component of the incident field of (22) tangential to the surface of the scatterer and testing with the functions of (13). The resulting expressions for the azimuthal mode m are shown below. In these expressions, B_m refers to Bessel function of the first kind of order m.

$$E_{t\ mq}^{\theta^{inc}} = E^{\theta^{inc}} \pi e^{-jm\phi^{inc}} \sum_{f=1}^{F} \rho_{q-1/2} T_t^q(t_{f-1/2}) e^{jkz_{q-1/2}\cos\theta^{inc}} \cdot$$

$$[\ \cos\theta^{inc}\sin\gamma_f\{j^{m+1}B_{m+1}(k\rho_{f-1/2}\sin\theta^{inc})+j^{m-1}B_{m-1}(k\rho_{f-1/2}\sin\theta^{inc})\}$$

$$-\sin\theta^{inc}\cos\gamma_f\{2j^mB_m(k\rho_{f-1/2}\sin\theta^{inc})\}\ ] \qquad (24a)$$

$$q = 1, .., N_t$$

$$E_{t\ mq}^{\phi^{inc}} = -E^{\phi^{inc}} \pi e^{-jm\phi^{inc}} \sum_{f=1}^{F} \rho_{f-1/2} T_t^q(t_{f-1/2}) e^{jkz_{f-1/2}\cos\theta^{inc}} \cdot$$

$$\sin\gamma_{f-1/2}j^m\{B_{m+1}(k\rho_{f-1/2}\sin\theta^{inc})+B_{m-1}(k\rho_{f-1/2}\sin\theta^{inc})\} \qquad (24b)$$

$$q = 1, .., N_t$$

$$E_{\phi\ mq}^{\theta^{inc}} = E^{\theta^{inc}} \pi e^{-jm\phi^{inc}} \sum_{f=1}^{F} \rho_{f-1/2} T_\phi^q(t_{f-1/2}) e^{jkz_{f-1/2}\cos\theta^{inc}} \cdot$$

$$\cos\theta^{inc}j^m\{B_{m+1}(k\rho_{f-1/2}\sin\theta^{inc})+B_{m-1}(k\rho_{f-1/2}\sin\theta^{inc})\} \qquad (24c)$$

$$q = 1, .., N_\phi$$

$$E_{\phi\ mq}^{\phi^{inc}} = E^{\phi^{inc}} \pi e^{-jm\phi^{inc}} \sum_{f=1}^{F} \rho_{f-1/2} T_\phi^q(t_{f-1/2}) e^{jkz_{f-1/2}\cos\theta^{inc}} \cdot$$

$$\{j^{m+1}B_{m+1}(k\rho_{f-1/2}\sin\theta^{inc})+j^{m-1}B_{m-1}(k\rho_{f-1/2}\sin\theta^{inc})\} \qquad (24d)$$

$$q = 1, .., N_\phi$$

In the case of sub-domain expansion/testing scheme, we can simplify the summations of (24) because the testing functions are confined to a small part of the scatterer.

Summation over the modes

The expressions for the matrix elements and forcing functions given in (15) and (24) are for a single azimuthal mode m. To obtain a solution to the scattering problem, one needs to sum over a finite number of modes from $-M$ to M. The value of M is determined by several factors such as the size of the scatterer and the angle of incidence of the excitation. Usually the fatter (large ρ) a scatterer, the larger the number of modes required. When the excitation is axially incident, the only modes excited are 1 and -1. The farther the excitation is away from the axial direction, the more the number of modes required to obtain a solution. A rule of thumb given by [3] is

$$M \simeq k\rho_{max}\sin\theta^{inc}+6$$

where ρ_{max} is the maximum radial dimension of the scatterer. This rule is valid only if $k\rho_{max}\sin\theta^{inc}$ is greater than about 3.

The expressions for the matrix elements and the forcing functions depend on the mode number m. This dependence is such that the following relationships between the moment matrix of the positive modes and those of the corresponding negative modes are valid.

$$\begin{bmatrix} \beta^m_{..} & \beta^m_{..} \\ \beta^m_{..} & \beta^m_{..} \end{bmatrix} = \begin{bmatrix} \beta^m_{..} & -\beta^m_{..} \\ -\beta^m_{..} & \beta^m_{..} \end{bmatrix}$$

Similarly, the forcing functions are related as follows.

$$\begin{bmatrix} E_{tm}^{\theta^{inc}} \\ E_{\phi m}^{\theta^{inc}} \end{bmatrix} = \begin{bmatrix} E_{t-m}^{\theta^{inc}} \\ -E_{\phi-m}^{\theta^{inc}} \end{bmatrix}$$

$$\begin{bmatrix} E_{tm}^{\phi^{inc}} \\ E_{\phi m}^{\phi^{inc}} \end{bmatrix} = \begin{bmatrix} -E_{t-m}^{\phi^{inc}} \\ E_{\phi-m}^{\phi^{inc}} \end{bmatrix}$$

In the above, the superscripts denote the component of incident field and the subscripts denote local coordinates on the scatterer. This relationship between the forcing functions and matrix elements of positive and negative modes lead to the following relationship between the coefficients of equivalent current.

$$\begin{bmatrix} J_{tm}^{\theta^{inc}} \\ J_{\phi m}^{\theta^{inc}} \end{bmatrix} = \begin{bmatrix} J_{t-m}^{\theta^{inc}} \\ -J_{\phi-m}^{\theta^{inc}} \end{bmatrix}$$

$$\begin{bmatrix} J_{tm}^{\phi^{inc}} \\ J_{\phi m}^{\phi^{inc}} \end{bmatrix} = \begin{bmatrix} -J_{t-m}^{\phi^{inc}} \\ J_{\phi-m}^{\phi^{inc}} \end{bmatrix}$$

Again, the superscripts denote to the component of incident field that is producing the currents. Because of this relationship between coefficients of current for the positive and negative modes, we need to calculate the currents of the positive modes.

Computation of Radar Cross-section

The scattered fields can be computed as the radiation field field from the equivalent surface currents. Using reciprocity [1], the expressions for this field can be written as

$$\mathbf{E} \cdot \hat{\mathbf{u}} = \frac{-j\omega\mu}{4\pi} \frac{e^{-jkR}}{R} \int\int \mathbf{E}^{r} \cdot \mathbf{J} \; dS \qquad (25)$$

where $\mathbf{E}^{r}$ is the field due to a test source located at the observation point with its amplitude adjusted to produce a unit plane wave at the origin, and polarized in the direction of $\mathbf{u}$. Thus,

$$\mathbf{E}^{r} = \hat{\mathbf{u}} e^{-j\mathbf{k}\cdot\mathbf{r}} \qquad (26)$$

For the moment solution where current is given as a summation of the product of the basis functions B_n and corresponding coefficients I_n, (25) can be written as

$$\mathbf{E} \cdot \hat{\mathbf{u}} = \frac{-j\omega\mu}{4\pi} \frac{e^{-jkR}}{R} [R][I] \qquad (27a)$$

where

$$[R] = \left[\int\int \mathbf{B}_n \cdot \mathbf{E}^{r} dS \right] \qquad (27b)$$

the integration being carried out over the surface of the scatterer. In the above, (27b) has exactly the same form as that used for the forcing function vector discussed earlier, the only difference being the basis functions $\mathbf{B_n}$ replacing the testing functions $\mathbf{T_q}$. Since we are using Galerkin's procedure, the basis and testing functions are conjugates of one another. Hence the expressions for the vector [R] are obtained from the expressions for the forcing function given in (24) by replacing the angles θ^{inc} and ϕ^{inc} with the corresponding observation angles and changing the mode number m to −m to account for the conjugation.

Observe that in (24) we have broken up an arbitrarily polarized incident plane wave into two linearly polarized plane waves. In terms of these components the scattered field components can be written as

$$
\begin{bmatrix} E_\theta^s \\ E_\phi^s \end{bmatrix} = \frac{-j\omega\mu}{4\pi} \frac{e^{-jkR}}{R} \begin{bmatrix} s^{\theta\theta} & s^{\theta\phi} \\ s^{\phi\theta} & s^{\phi\phi} \end{bmatrix} \begin{bmatrix} E_\theta^i \\ E_\phi^i \end{bmatrix}
\tag{28}
$$

The elements of the scattering matrix are obtained by summing the contributions due to the various azimuthal modes as

$$
s^{uv} = \sum_{m=-\infty}^{\infty} s_m^{uv}
\tag{29}
$$

uv being $\theta\theta$, $\theta\phi$, $\phi\theta$, or $\phi\phi$. The terms under the summation are obtained as shown below.

$$
s_m^{uv} = [[R_{t\ m}^u]\ [R_{\phi\ m}^u]] \begin{bmatrix} J_{t\ m}^v \\ J_{\phi\ m}^v \end{bmatrix}
\tag{30a}
$$

$$
= [[R_{t\ m}^u]\ [R_{\phi\ m}^u]] \begin{bmatrix} \beta_{11}^m & \beta_{12}^m \\ \beta_{21}^m & \beta_{22}^m \end{bmatrix}^{-1} \begin{bmatrix} E_{t\ m}^v \\ E_{\phi\ m}^v \end{bmatrix}
\tag{30b}
$$

The elements of the various R's used here are obtained from the expressions for the E's of (24) by replacing θ^{inc} and ϕ^{inc} with the corresponding observation angles and changing the mode number m to $-m$. Once the scattered field has been computed, the radar cross-section defined as

$$\sigma^{uv} = 4\pi r^2 \left| \frac{E_u^{scat}}{E_v^{inc}} \right|^2 \tag{31a}$$

is easily computed. Using (28), this can be written in terms of the elements of the scattering matrix as

$$\sigma^{uv} = 4\pi \left| s^{uv} \right|^2 \tag{31b}$$

This can easily be extended ([4]) to arbitrarily polarized transmitters and receivers.

NUMERICAL RESULTS

In this section, sample results obtained using the sub-domain basis set is compared with those obtained using entire-domain basis set.

First, a conducting sphere illuminated by a plane wave polarized in the x direction and travelling in the -z direction as shown in Fig. 5a is considered. The radius of the sphere is 1 wavelength. The pulse basis set solution is obtained by modeling the generating arc using 31 linear segments. This results in approximately 10 sub-sections per wavelength. (This is the recommended density for sub-sectional basis functions). This results in a 61 by 61 matrix equation. For the entire domain basis set, the scatterer is modeled using the same number of linear segments as in the pulse basis set, but the number of basis functions used is 11 for J_t (and 13 for J_ϕ). This is approximately 4 basis functions per wavelength and is the recommended density of basis functions for most scatterers when using entire domain basis functions.

Since the excitation in this case is axial, the only modes excited are 1 and -1. As discussed earlier, only the positive numbered modes are computed, since the solution for the corresponding negative numbered modes can be algebraically derived from the positive mode solutions.

Fig. 6 shows the comparison of bistatic scattering cross-section for this sphere computed using the two methods. The two solutions are very close to each other. Table 1 compares the computation times required for each method. The time used by the entire-domain program is about twice that required for the sub-domain program.

Fig. 7 shows the comparison of bistatic scattering cross-section of the open-ended cylinder problem shown in Fig. 5b. The cylinder is 4 wavelengths long and the matrix sizes used follow the rule of thumb of 10 basis functions per wavelength for sub-domain case and 4 basis functions for the entire domain case. Again, as illustrated by the numbers in Table 1, the entire domain program results achieves a savings in the matrix size, but at the expense of more computer time.

DESCRIPTION OF PROGRAMS

Two programs, referred to here as PBOR and GBOR have been developed to solve the conducting body of revolution scattering problem. PBOR uses the pulse basis set and GBOR uses the entire domain basis set. Both program require the LINPACK library routines CGECO, CGESL and CGEDI. The input data is read from a file. The file name is requested by the program during execution. The output is written to two files whose names also are requested by the program. Notice that the input data required by the two programs are different.

The format of input data for PBOR is shown below.

```
NFLDS,   WVL
THETA, PHI, ETHETA, ETH-PHASE, EPHI, EPH-PHASE, NOBS
OBST,OBSP
.........
THETA, PHI, ETHETA, ETH-PHASE, EPHI, EPH-PHASE, NOBS
OBST,OBSP
.........
................................................
.........
.........
RHO,Z
....
```

The first line of input data should have the number of different excitations (NFLDS) and the wavelength of the incident excitation(s). Following this, there should be NFLDS lines of incident field data with each line having the spherical coordinate angles (in degrees) of incidence THETA and PHI, the magnitude (ETHETA) and phase (ETH-PHASE) in degrees, of the theta component of this excitation, the magnitude (EPHI) and phase (EPH-PHASE) in degrees, of the phi

component of the excitation, and number of observation points (NOBS) at which the far-fields and scattering cross-section are to be computed for this excitation. After this, there should be NOBS lines of observation point data with each line containing the observation angles theta (OBST) and phi (OBSP). Repeat this set of incident field data and observation point data as many times as there are incident excitations. Finally, there should be as many lines of RHO and Z coordinate points as required to describe the scatterer. These points are connected end to end using straight lines to obtain an approximation to the generating arc.

The format of the input data set for GBOR is shown below.

```
NFLDS, NOBS, N, WVL
THETA, PHI, ETHETA, ETH-PHASE, EPHI, EPH-PHASE
. . . . .
OBST,OBSP
. . . . .
RHO,Z
. . . .
```

This format of input data for GBOR is somewhat different from that of PBOR. The number N indicates the number of basis functions that should be used. It should be such that there are approximately 4 basis functions per wavelength. The number of observation points are taken to be the same for all the excitations. Thus, starting at the second line, there should be NFLDS lines of incident field data and following this NOBS lines of observation point data.

ACKNOWLEDGMENTS

REFERENCES

1. Harrington, R.F.,"*Time harmonic electromagnetic fields*," McGraw Hill, New York, NY. 1961.

2. Glisson, A.W. and D.R. Wilton,"*Simple and efficient numerical techniques for treating bodies of revolution*," Tech. Rep. 105, Univ. of Mississippi, 1979.

3. Andreasen, M.G., "*Scattering from bodies of revolution*," IEEE *Trans. Ant. Propagat.*, pp303-310, March, 1965.

4. Mautz, J.R. and R.F. Harrington, "Radiation and scattering from bodies of revolution," *Appl.Sci. Res.*, pp 405-435, vol. 20, June 1969.
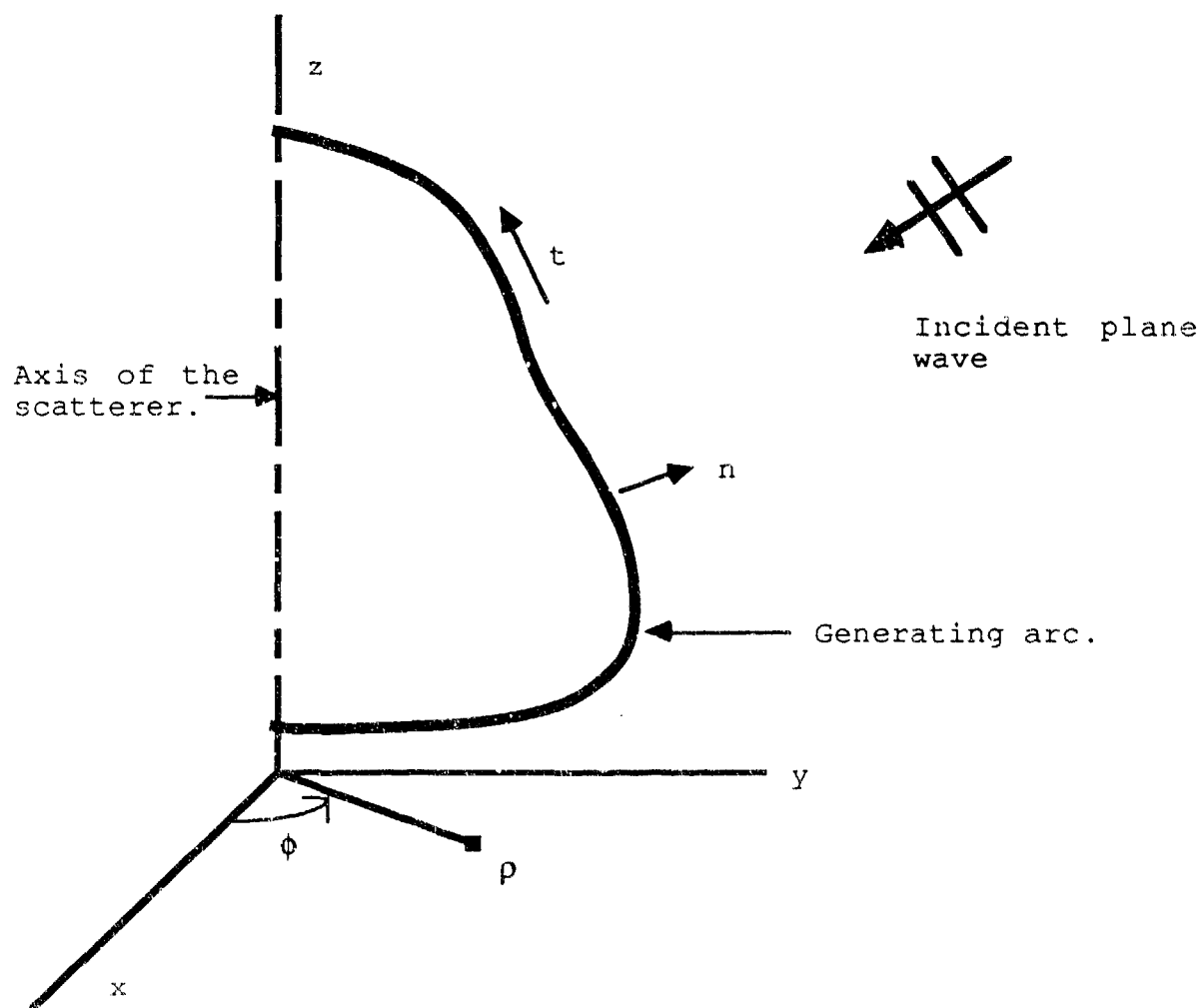
Fig. 1 Geometry of the body of revolution problem.
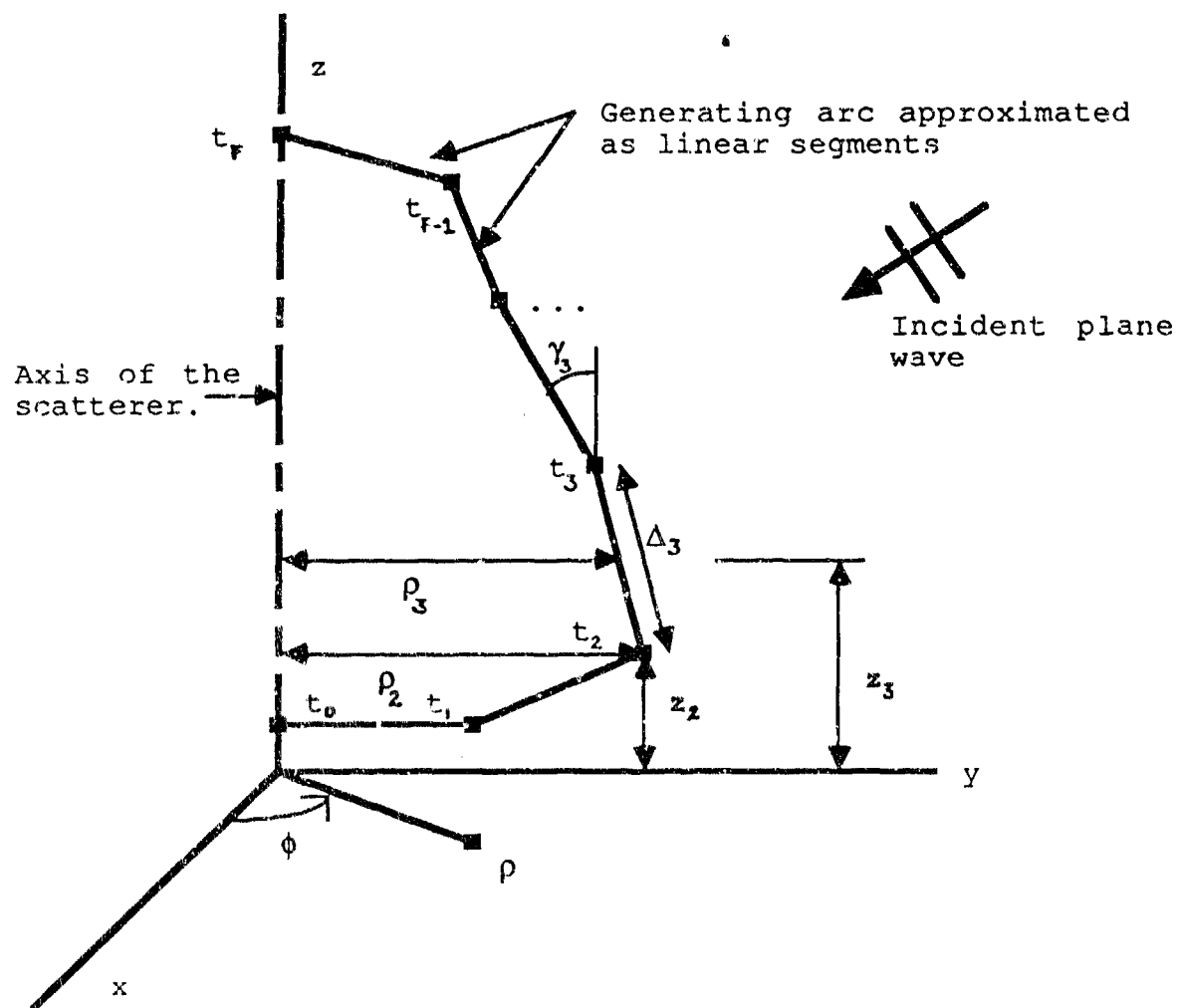
Fig. 2 Discretization of the body of revolution problem.
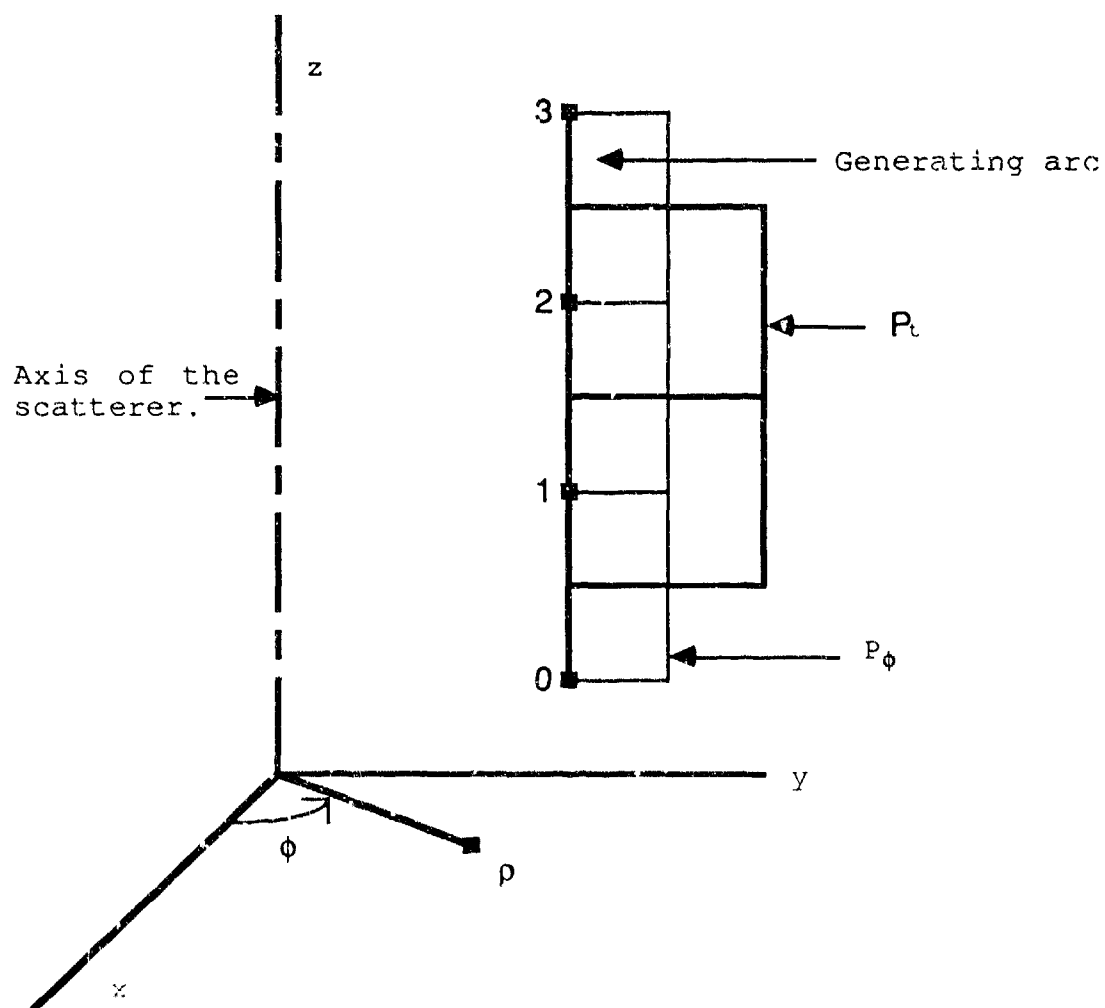
Fig. 3 Positioning of P_t's and P_ϕ's on a generating arc modeled by three linear segments. There are 3 P_ϕ's and 2 P_t's.
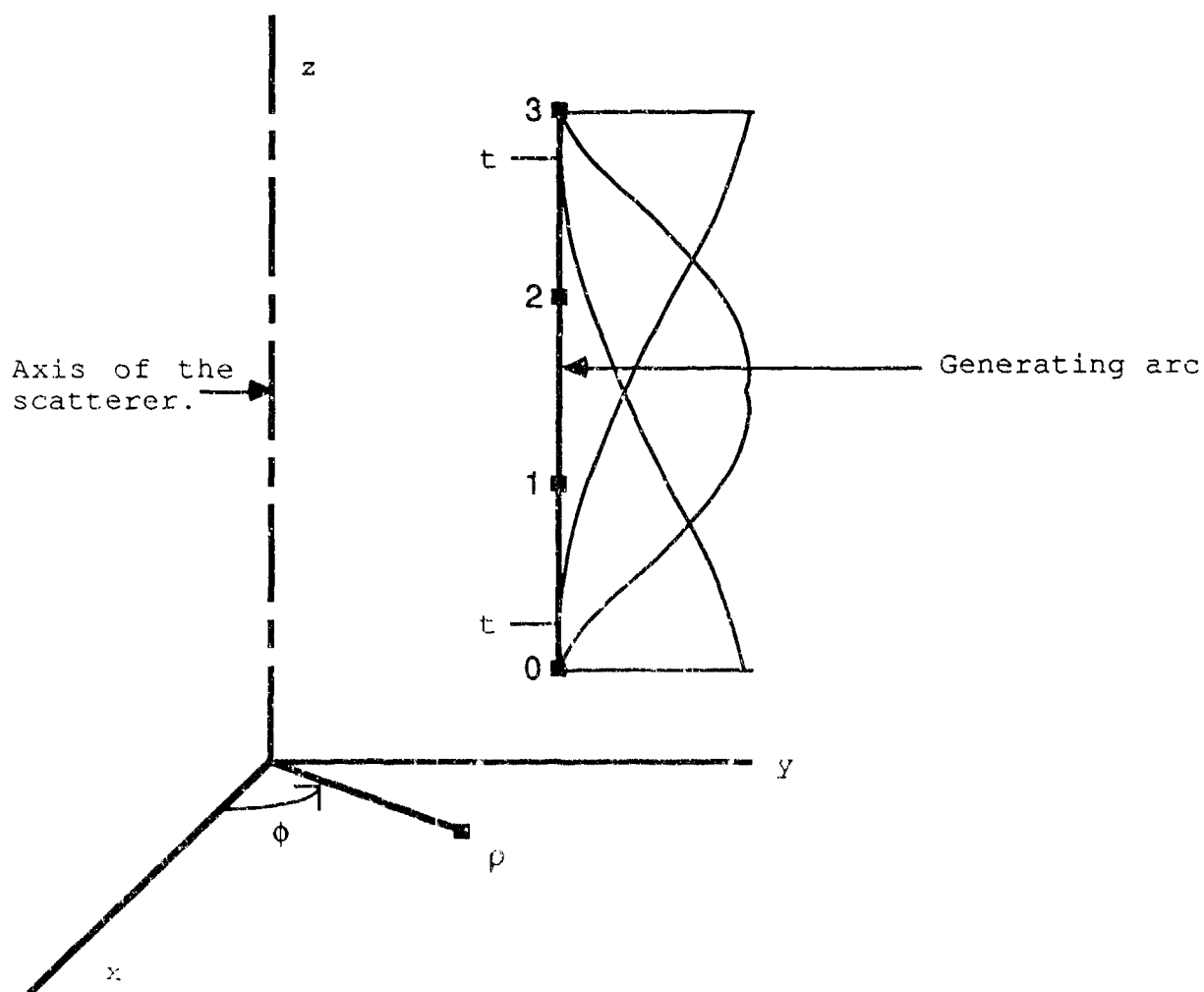
Fig. 4 Positioning of Gaussian basis functions on a generating arc modeled using 3 linear segments. Three basis functions are shown. The half-gaussian functions are used only for the phi component of current. Note that there is no relation between the number of linear segments and the number of basis functions.
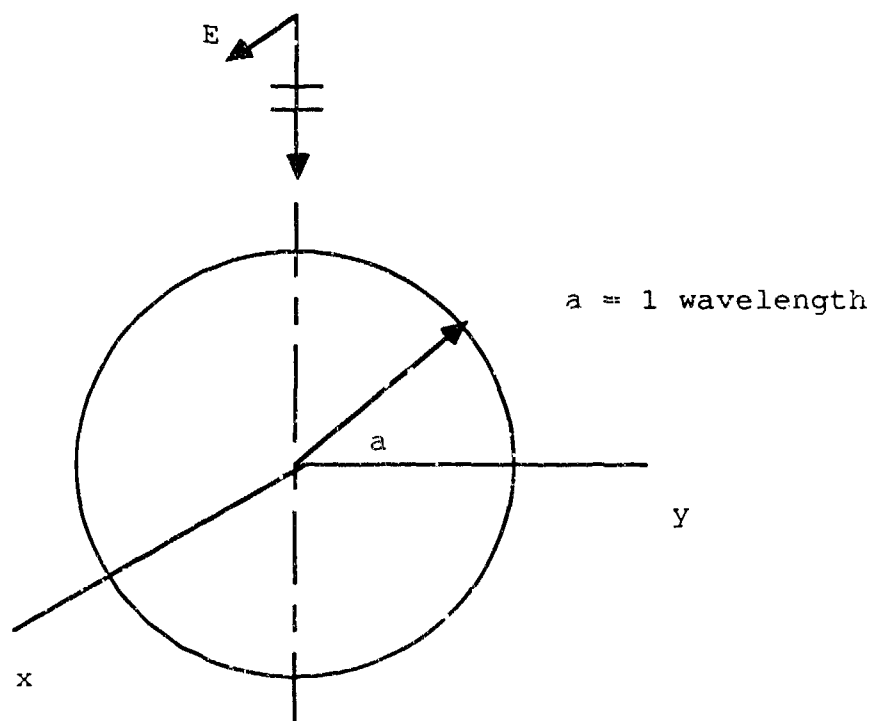
Fig 5a. Conducting sphere used as a test case for results
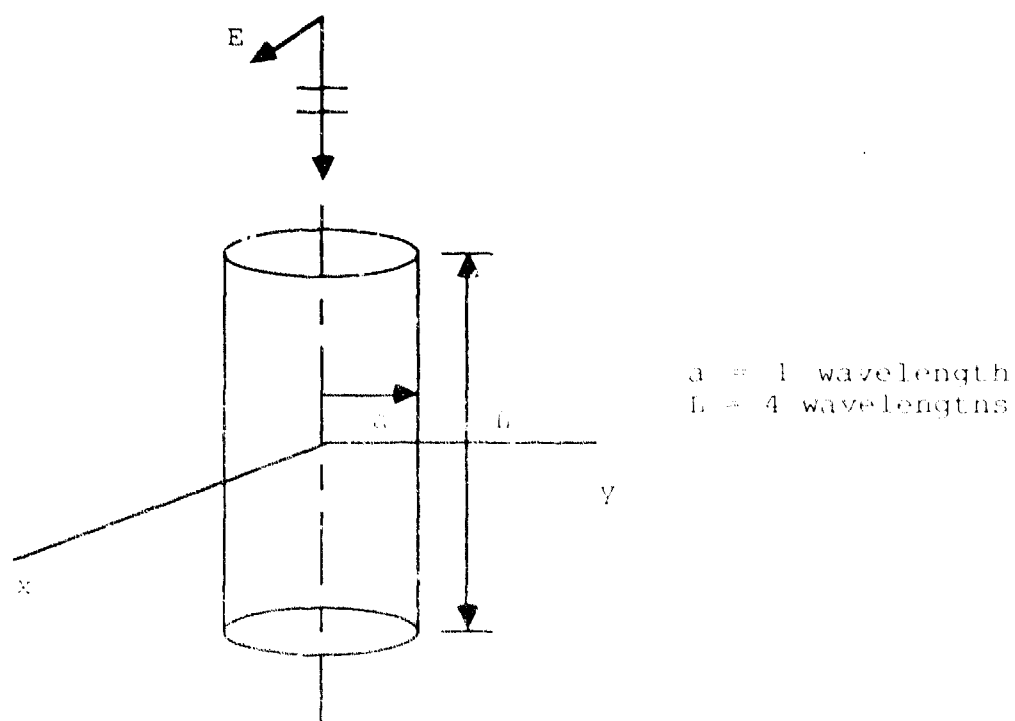presented in Fig. 6.

Fig. 5b. Conducting cylinder used to compute results
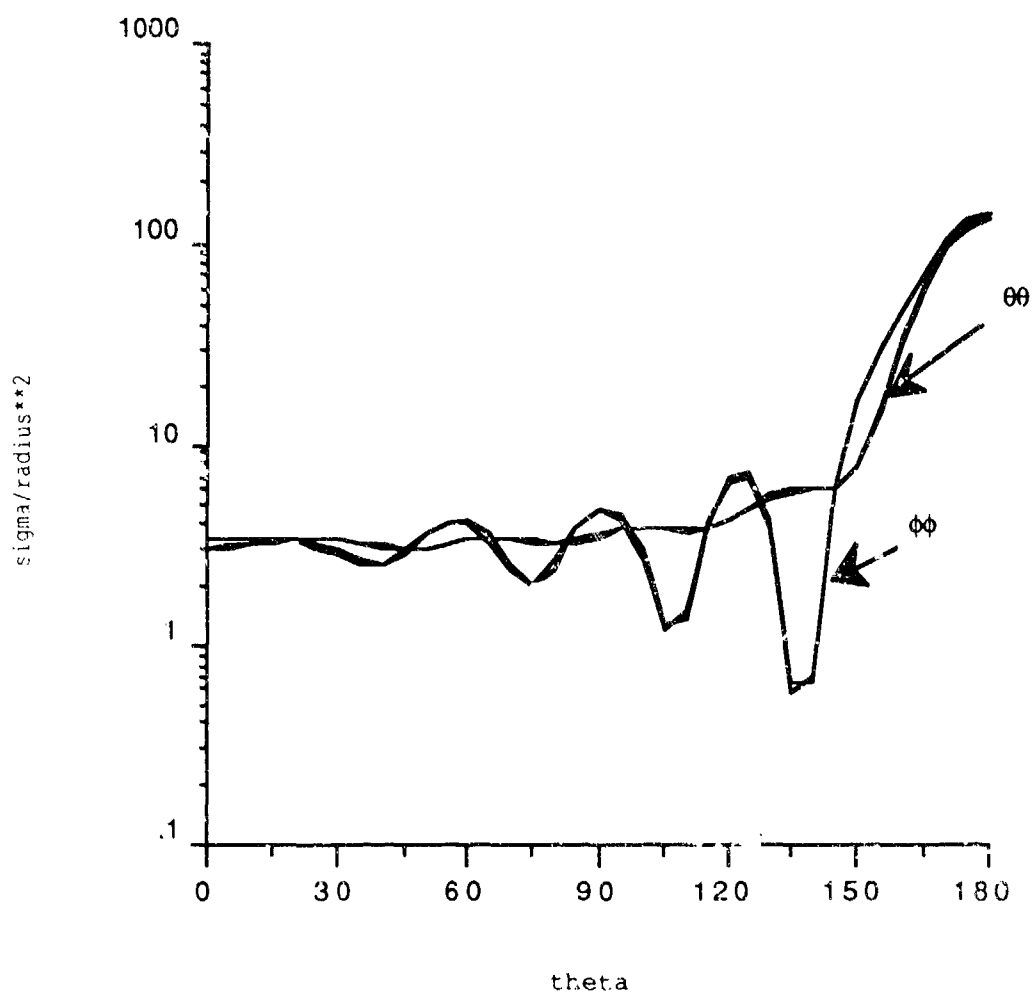presented in Fig. 7.

Fig. 6: Bistatic scattering cross-section of the conducting
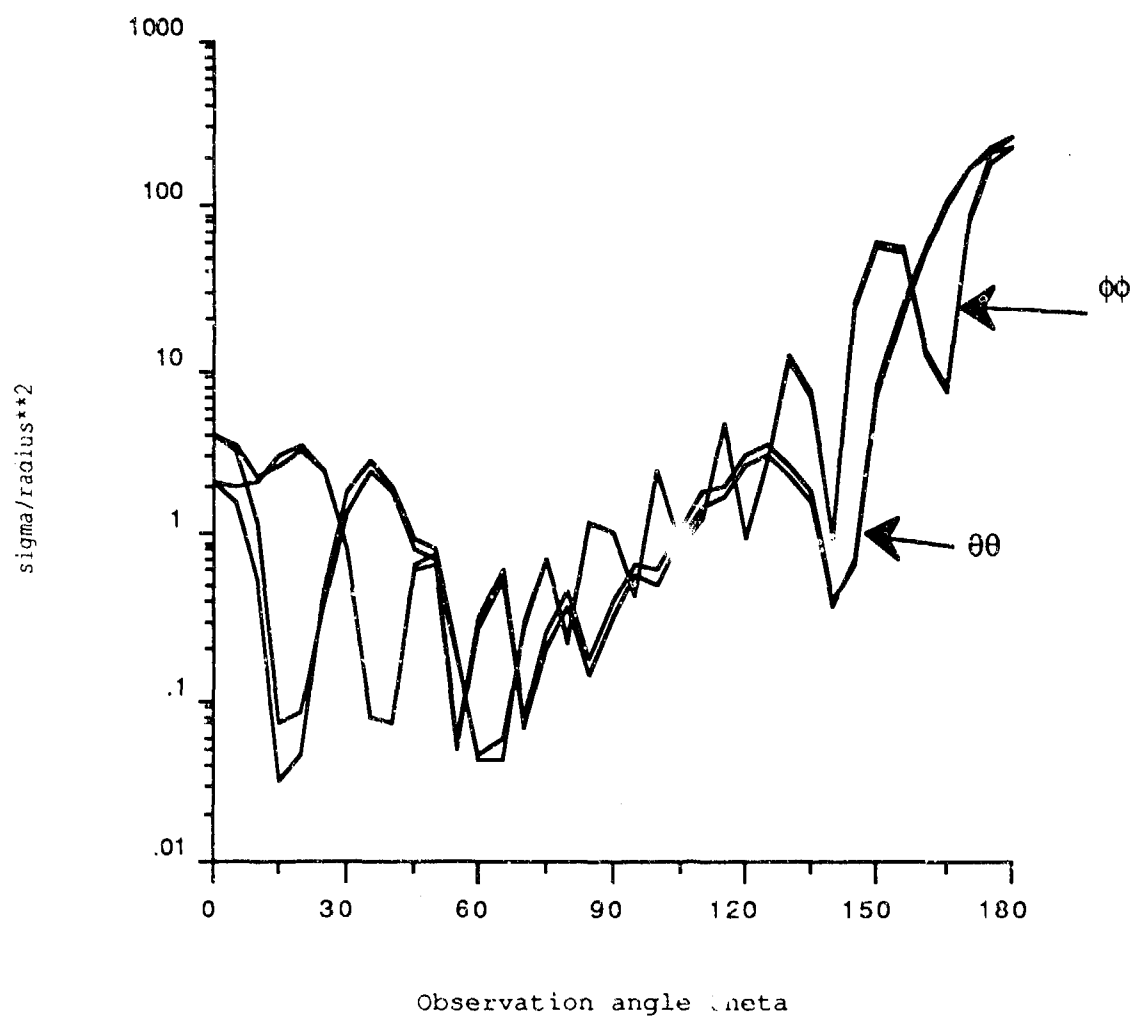sphere illustrated in Fig. 5a.

Fig. 7: Bistatic scattering cross-section of conducting cylinder of Fig. 5b.

Scatterer	Length of generating arc in wavelengths	Matrix size		Computation time in cpu seconds on cray xmp-48	
		Sub domain	Entire domain	Sub domain	Entire domain
Sphere	3.14159	61	24	7.834	15.385
Cylinder	4.0	81	34	8.061	17.181

Table 1. Comparison of computation times and matrix sizes for scattering problems using entire domain basis functions and sub-domain basis functions.